THE JOURNAL OF BIOLOGICAL CHEMISTRY
Vol. 278, No. 8, Issue of February 21, pp. 6516–6520, 2003
Printed in U.S.A.

Crystal Structure of Human Protein-tyrosine Phosphatase SHP-1*

Received for publication, October 11, 2002, and in revised form, December 4, 2002
Published, JBC Papers in Press, December 13, 2002, DOI 10.1074/jbc.M210430200

Jian Yang‡§, Lijun Liu‡, Dandan He‡, Xi Song‡, Xiaoshan Liang‡, Zhizhuang Joe Zhao¶, and G. Wayne Zhou‡‖

From the ‡Program in Molecular Medicine, University of Massachusetts Medical School, Worcester, Massachusetts 01605 and the ¶Department of Medicine, Vanderbilt University, Nashville, Tennessee 37232

SHP-1 is a cytosolic protein-tyrosine phosphatase that behaves as a negative regulator in eukaryotic cellular signaling pathways. To understand its regulatory mechanism, we have determined the crystal structure of the C-terminal truncated human SHP-1 in the inactive conformation at 2.8-Å resolution and refined the structure to a crystallographic *R*-factor of 24.0%. The three-dimensional structure shows that the ligand-free SHP-1 has an auto-inhibited conformation. Its N-SH2 domain blocks the catalytic domain and keeps the enzyme in the inactive conformation, which supports that the phosphatase activity of SHP-1 is primarily regulated by the N-SH2 domain. In addition, the C-SH2 domain of SHP-1 has a different orientation from and is more flexible than that of SHP-2, which enables us to propose an enzymatic activation mechanism in which the C-SH2 domains of SHPs could be involved in searching for phosphotyrosine activators.

Tyrosine phosphorylation is a key mechanism for regulating eukaryotic cellular signaling pathways. The protein tyrosine phosphorylation level is precisely regulated by two types of enzymes: protein-tyrosine kinases (PTKs)[1] and protein-tyrosine phosphatases (PTPs), in which PTPs act to counter-balance the process through dephosphorylation of the phosphorylated tyrosines (1, 2). PTPs can be divided into two groups, receptor protein-tyrosine phosphatases and cytosolic protein-tyrosine phosphatases. The SH2 domain-containing PTPs, SHP-1 and SHP-2, are both cytosolic PTPs and share many structural and regulatory features. They both have two tandem SH2 domains at the N terminus followed by a single catalytic domain and an inhibitory C-terminal tail. However, irrespective of similar structural and regulatory characteristics, these two enzymes have different biological function *in vivo*.

Different from SHP-2, which is expressed in all kinds of tissues, SHP-1 is predominantly expressed in hematopoietic and epithelial cells and behaves mainly as a negative regulator of signaling pathways in lymphocytes (1, 2). SHP-1 is dormant in the cytosol, with its phosphatase activity inhibited by both the SH2 domains and the C-terminal tail (1, 3–5). In response to an activation signal, SHP-1 is recruited to membrane-bound inhibitory receptors via the binding of its SH2 domains to the tyrosine-phosphorylated immunoreceptor tyrosine-based inhibitory motif within the cytoplasmic domain of a receptor (6–8). During this process, SHP-1 undergoes a structural rearrangement, exposes its active site, and binds to the downstream substrates, thereby dephosphorylating the substrates to turn off the cellular signals.

SHP-1 also presents in several types of non-hematopoietic cells (9–12). Overexpression of a catalytically inactive SHP-1 mutant in these cells strongly suppressed mitogen-activated pathways, reducing signal transduction and activation of transcription; these findings demonstrate that SHP-1 has a positive effect on mitogenic signaling in these non-hematopoietic cells (10, 11). Thus, SHP-1 probably has both the negative and positive regulatory function in different types of cells. Many aspects of the molecular mechanism that underlies the activation and regulation of SHP-1 remain unclear.

Here, we report the 2.8-Å crystal structure of the 61-residue C-terminal-truncated SHP-1 (residues 1–532) in the ligand-free dormant conformation. SHP-1 shares a 60% overall sequence identity with SHP-2. A comparison of the crystal structures of SHP-1 and SHP-2 reveals that the C-SH2 domain of SHPs is highly mobile, suggesting that this domain may be involved in searching for phosphopeptides to activate the enzyme in the initial stages of enzyme activation.

EXPERIMENTAL PROCEDURES

Protein Expression, Purification, and Crystallization—The 61-residue C-terminal-truncated SHP-1 (residues 1–532) was cloned and expressed as described previously (13), except that the *Escherichia coli* strain of BL21 (pLysS) was used for the expression to increase the protein solubility. Purification was operated by ion exchange and affinity chromatography. The harvested protein sample was desalted by centrifugation and concentrated to 3 mg ml^{-1} for crystallization. Crystallization was performed by the vapor-diffusion hanging-drop method at 4 °C. The crystallization drops composed of equal-volume mixture (3 μl:3 μl) of protein solution and reservoir solution (25–30% polyethylene glycol 8000, 5 mM dithiothreitol, 0.1 M HEPES, pH 7.0) were equilibrated against the reservoir solution (0.5 ml), and crystals were obtained within 2 weeks.

Data Collection and Structural Determination—A 2.8-Å diffraction data set was collected at 100 K on the F1 beamline at CHESS (Cornell University). The x-ray wavelength was 0.978 Å. 15% glycerol was introduced into the reservoir solution as cryoprotectant to reduce the freezing damage to crystals. Data were processed with DENZO and SCALEPACK (14). The space group of the SHP-1 crystals belongs to $P2_12_12_1$, and the unit-cell parameters were determined to be a = 44.74 Å, b = 100.40 Å, and c = 149.47 Å. There was one molecule per asymmetric unit.

The structure of SHP-1 was solved by the molecular replacement method with AmoRe (15), using the coordinates of C-terminal truncated

* This work was supported by a Career Development Award from the American Diabetes Association (to G. W. Z.), the Pilot project from Diabetes and Endocrinology Research Center program of the University of Massachusetts Medical School (to G. W. Z.), and by National Institutes of Health Grants AL45858 (to G. W. Z.) and HL57393 and CA75218 (both to Z. J. Z.). The costs of publication of this article were defrayed in part by the payment of page charges. This article must therefore be hereby marked "*advertisement*" in accordance with 18 U.S.C. Section 1734 solely to indicate this fact.

§ Current address: Rosenstiel Basic Medical Sciences Research Center, Brandeis University, 415 South St., Waltham, MA 02454.

‖ To whom correspondence should be addressed: Program in Molecular Medicine, University of Massachusetts Medical School, 373 Plantation St., Worcester, MA 01605. Tel.: 508-856-6869; Fax: 508-856-1218; E-mail: wayne.zhou@umassmed.edu.

[1] The abbreviations used are: PTK, protein-tyrosine kinase; PTP, protein-tyrosine phosphatase; SH2, src homology 2; r.m.s., root mean square; CSW, PTP2.

TABLE I
Data collection and refinement characteristics for SHP-1

Data collection	
Beamline	F1 in CHESS
Wavelength (Å)	0.978
Space group	$P2_12_12_1$
Unit cell constants (Å)	$a = 44.74$, $b = 100.40$, $c = 149.47$
Resolution range (Å)[a]	50–2.80 (2.95–2.80)
Total reflections observed	63,500
Unique reflections	12,921
Completeness (%)	96.7 (89.9)
$I/\sigma(I)$	5.1 (2.0)
R_{merge} (%)	9.9 (31.5)
Refinement	
Resolution range (Å)	10.0–2.8
Data cutoff ($F/\sigma(F)$)	2
R-free (%)[b]	33.4
R-factor (%)	24.0
r.m.s. deviation for bond lengths (Å)	1.43
r.m.s. deviation for bond angles (°)	0.007

[a] Numbers in parentheses indicate outer shell values.
[b] 10% of the diffraction were randomly selected as a test set for calculation of the R-free factor.

SHP-2 (16) as the search model. Refinement was performed with CNS (17). The refinement process was monitored with the free R-factor that was calculated using randomly selected 10% of the data as the test set. After the initial rigid-body refinement, a $2F_o - F_c$ electron density map was calculated. The C-SH2 domain was found to apparently mismatch the first $2F_o - F_c$ map. Therefore, the C-SH2 domain was omitted from the model. Thereafter, five cycles of positional refinement and re-building the model for the N-SH2 and PTP domains were applied for all data in the resolution range of 10–3.0 Å, and an $F_o - F_c$ map was generated. Subsequently, the C-SH2 domain was manually re-assigned based on the omitted $F_o - F_c$ map. The full model was refined with the 2-σ cutoff data in the 10–2.8-Å resolution range. The model building interspersed with CNS refinement was done with TURBO-FRODO (18). In the penultimate cycle, the free R-factor was reduced to 33.4%, correspondingly, the final crystallographic R-factor was 24.0%, with all reflections used in the refinement. In the final model, the linker regions between the C-SH2 domain and the N-SH2 and catalytic domains were not observed. No water molecules were assigned to the final model. The crystal statistics, final refinement results, and geometric analyses are summarized in Table I.

RESULTS AND DISCUSSION

Overall Structure of SHP-1—The crystallized ligand-free human protein-tyrosine phosphatase SHP-1 contains residues 1–532 but lacks the 61-residue C-terminal tail. Its crystal structure has been determined by molecular replacement method and refined to a final crystallographic R-factor of 24.0% at 2.8-Å resolution. The statistics for the crystal data and refinement results are shown in Table I.

Three domains were defined well from the present crystal structure. The residues 1–108 and 116–208 fold as two Src homology 2 domains, the N-SH2 and C-SH2 domains, respectively. Residues 270–532 fold as the typical PTP domain, a highly twisted ten-stranded β-sheet flanked by four helices on the convex side and two helices and a β-hairpin from the concave side. The N-terminal extended region of the PTP domain comprising helices α0 and α1′ are defined well, whereas the linker regions of C-SH2 to N-SH2 and to PTP domains, residues 109–115 and 209–231, were disordered and not observed on the finial electron density map. The architecture of the three domains is compact. The two SH2 domains look like two antennas of the global PTP domain in the overall view. Fig. 1 shows a ribbon representation of the final model (Fig. 1*A*), the intramolecular interaction at the interface between the N-SH2 and PTP domains (Fig. 1*B*), and a portion of an electron density map of the flexible C-SH2 domain (Fig. 1*C*). Fig. 2 shows the sequence alignment of SHP-1 with three of its homologues, with the secondary structure elements assigned.

Comparison of the SHP-1 Structure with the Domain-alone Structures—SH2 domain is responsible for recognizing the phosphotyrosine-containing proteins, thereby facilitating phosphorylation-dependent protein-protein interactions that result in signal propagation (19). In general, residue at the (p + 1) position of the phosphotyrosine peptide of the binding target is considered most important for defining the binding specificity (20). Crystal structure revealed that both SH2 domains of SHP-1 have the typical SH2 domain fold, which consists of a central four-stranded β-sheet with an α-helix on either side.

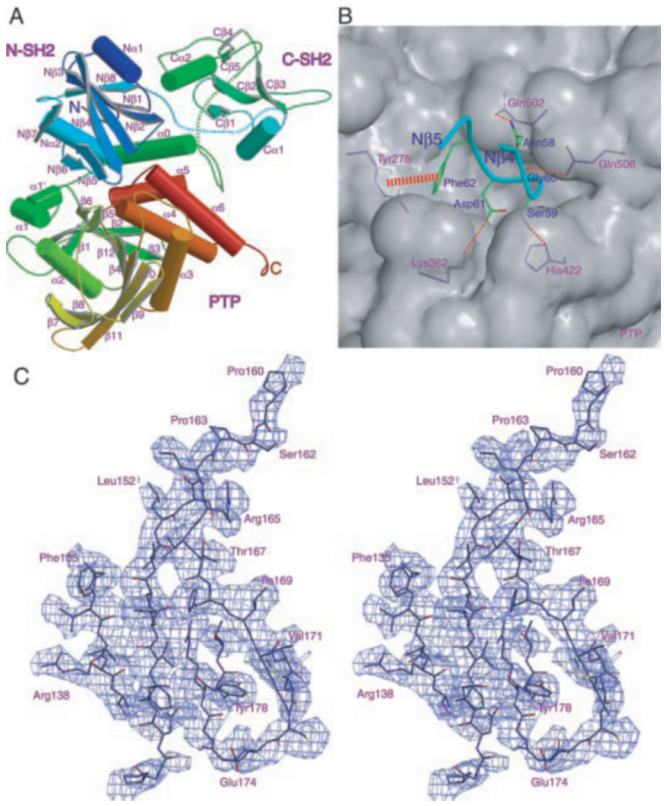

FIG. 1. **Overall structure of SHP-1.** A schematic drawing of the structure with the color ramping from *blue* (N-terminal) to *red* (C-terminal) is shown (*A*). The secondary structure elements are labeled according to the domains to which they belong. The *dashed lines* indicate disordered regions. The interactions between the Nβ4-Nβ5 hairpin loop of the N-SH2 domain and the active site of the PTP domain are shown by the accessible surface for the PTP domain and bonding models for the interactions (*B*). A stereo view of the $2F_o - F_c$ electron density map around the C-SH2 domain was contoured at 1.0 σ (*C*). These figures were prepared with MOLSCRIPT (31), RASTER3D (32), and GRASP (33).

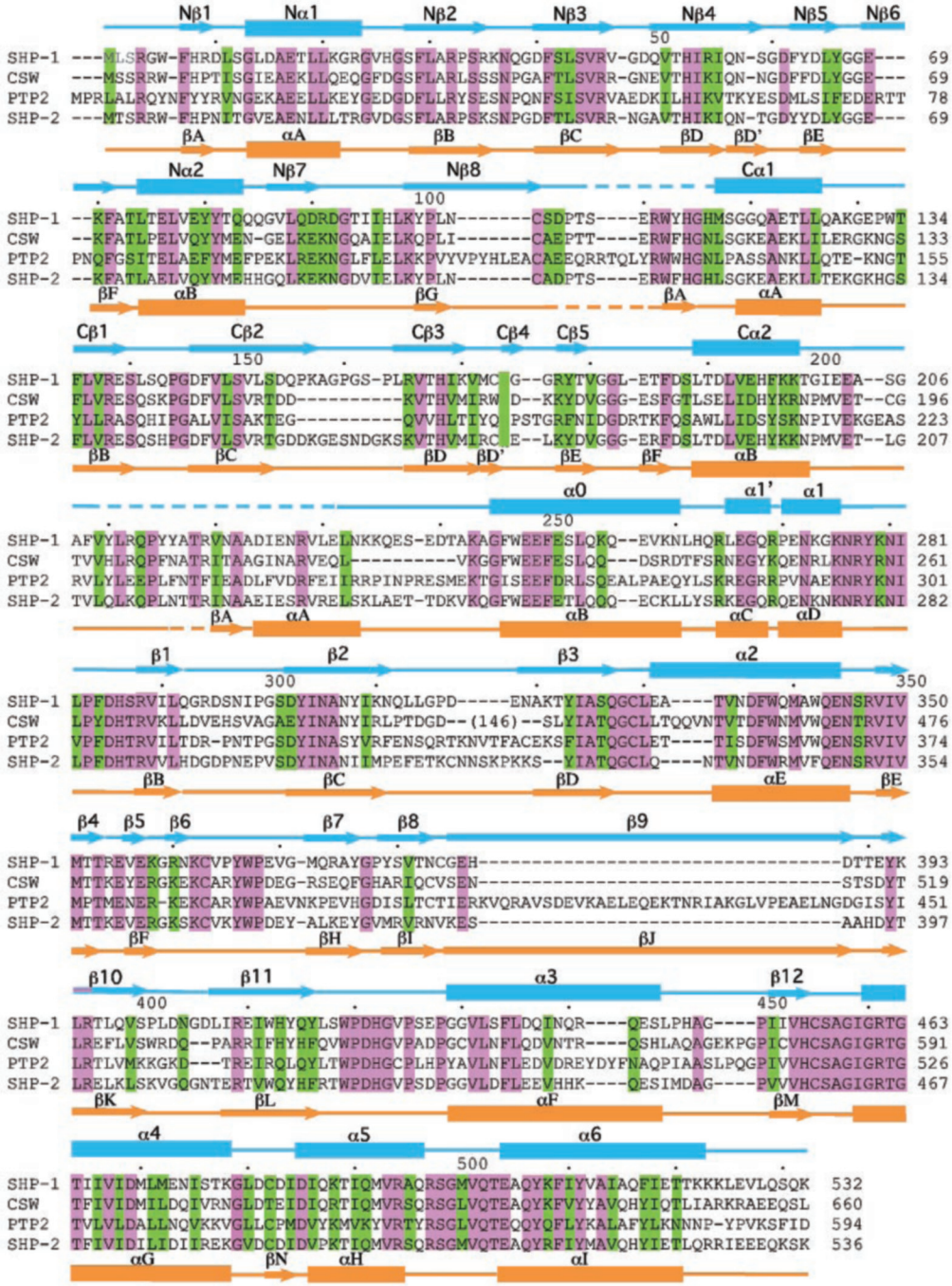

FIG. 2. **Sequence alignment and secondary structure element assignments for SHPs and their homologues.** Identical and similar residues are *cyan* and *green*, respectively. Secondary structure elements for SHP-1 and SHP-2 are shown in *blue* and *orange*, respectively.

The phosphopeptide-binding sites of both SH2 domains face away from the PTP domain and are fully exposed on the surface of the molecule (Fig. 3*A*). Nevertheless, the spatial arrangement of the two SH2 domains on PTP domain significantly differs. In contrast to the N-SH2 domain that strongly interacts with the PTP domain (see below), the C-SH2 domain is tethered around and extends to the surface of the catalytic domain and has no significant direct interactions with the PTP domain.

The structure of the PTP domain of ligand-free SHP-1 is almost identical to that of the peptide-bound catalytic domain of SHP-1 (Fig. 3*B*). Superimposition of the α-carbons between the structure of the auto-inhibited PTP domain and the previously reported structure of the catalytic domain of SHP-1 complexed with Tyr(P)^{469}-peptide (21) gives a root mean square (r.m.s.) deviation of 1.9 Å. Nevertheless, the conformations of the β5-β6 hairpin loops (residues 356–363) in these two structures significantly differ. In the present structure, the Cα of Gly^{359} in the β5-β6 loop is shifted 6.7 Å, reflecting an ~25-degree rotation of the hairpin's "plane" (Fig. 3*B*). It could be expected that the flexibility of this loop region was related to its important role in substrate recognition (21–23). Superimposition of these structures also shows flexibility around the phosphopeptide-binding sites of some other loops, with conformational changes of 1.5–2.0 Å for the α1-β1 and β3-α2 loops (Fig. 3*B*). In addition, the α0 helix appears to be highly mobile. In the Tyr(P)^{469}-PTP complex structure (21), the α0 is located at the N terminus, far away from the PTP domain. In the present SHP-1 structure, the α0 helix bridges the C-SH2 and PTP domains and rotates ~60 degrees to approach the surface of the PTP domain (Fig. 3*B*). This mobility reflects the high flexibility

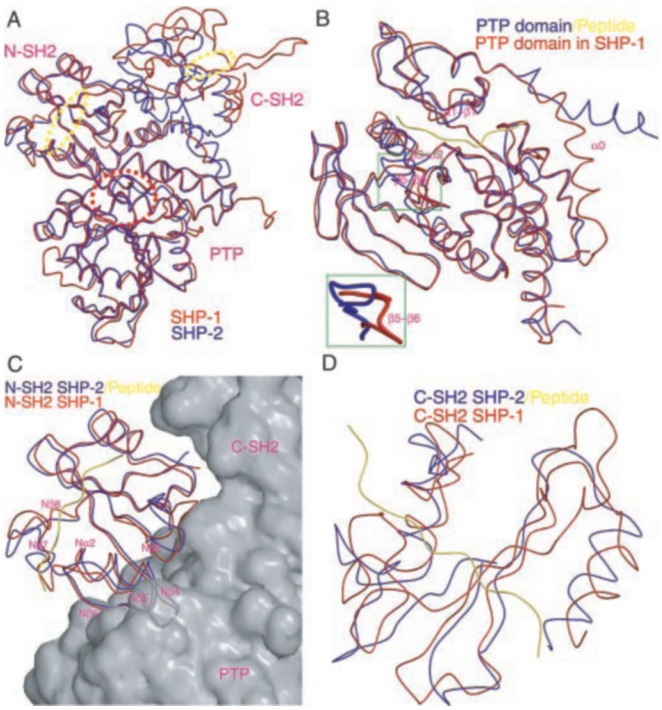

FIG. 3. **Structural comparison of SHP-1 and its domains with SHP-2 (*A*), the PTP domain (*B*) complexed with Tyr(P)^{469} (*yellow coil*) (21), and the N- and C-terminal SH2 domains (27) (*C* and *D*) of SHP-2.** All superimposition of the structures of SHP-1 and SHP-2 is based on the Cα atoms. The phosphopeptide-binding sites of the two SH2 domains and the active site of the PTP domain are indicated by the *yellow* and *red dashed ellipses*, respectively (*A*). The loop regions with large conformational changes are labeled, in which the conformational change of β5-β6 hairpin is highlighted in the *green box* (*B*). A part of the accessible surface is shown for the C-SH2 and PTP domains of SHP-1, and the loop regions with large conformational changes are labeled (*C*).

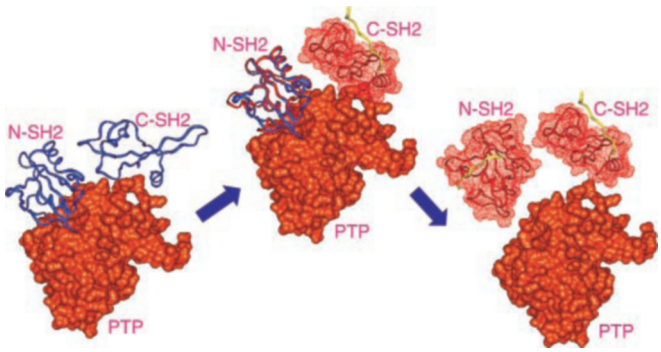

FIG. 4. **A proposed mechanism for the activation of SHP-1.** From *left* to *right*, the three structural models represent the auto-inhibited, C-SH2 domain-stimulated, and activated conformations. The molecular surface of the PTP domain is shown in *orange*. The SH2 domains modeled from SHP-1 and SHP-2 structures are depicted by *blue* and *red coils*, respectively. This figure was prepared with SETOR (34).

of the α0-α1 loop, which may be required for exposure of the active site during enzyme activation. Our previous research also lends support to the cooperative role of helix α0 in the substrate recognition (23).

Auto-inhibited Structure of SHP-1—Previous studies have revealed that both SH2 domains of SHP-1 could bind to tyrosine-phosphorylated immunoreceptor tyrosine-based inhibitory motif peptides (8). Similar to the crystallographic data for its close relative SHP-2, however, the crystal structure of the ligand-free SHP-1 supports that the N-SH2 domain, instead of C-SH2 or both domains, acts the auto-inhibition role. The interaction between N-SH2 domain and PTP domain is extensive, whereas the C-SH2 domain does not show significant interface with either of the other two domains.

Cys^{455}, the catalytic nucleophile, is located at the base of the active-site cleft. In the auto-inhibited conformation of SHP-1, it appears that the Nβ4-Nβ5 loop of the N-SH2 domain is protruding to the catalytic PTP domain to directly block the entrance to the active site, which prevents the cysteine residue from exposing to the substrate (Figs. 1*B* and 3*C*). This inactive conformation is stabilized by various interactions including the salt bridge between Asp^{61} and Lys^{362}, along with the π-π interaction between the Phe^{62} and Tyr^{278} side chains, and the hydrogen bonds in the residue pairs of Ser^{59}/His^{422}, Gly^{60}/Gln^{506}, and Asn^{58}/Gln^{502}. All of these amino acid residues involved in the interactions are conserved well between SHP-1 and SHP-2 except for Ser59; SHP-2 has a threonine residue at the corresponding site (Fig. 2). Likewise, most of these residues are also highly conserved in both CSW and PTP2 (Fig. 2), implying the similar interdomain interactions in these two enzymes. In addition, the extensive interactions around the protruding Nβ4-Nβ5 loop are present at the interface between the N-SH2 domain and the PTP domain (Fig. 3*C*). The area of interacting interface between these two domains is calculated to be 1478.9 Å^2, which is 20% larger than that in SHP-2.

In addition, the phosphopeptide-binding sites of both SH2 domains in SHP-1, like in SHP-2, appear to expose to the solvent but not to the active site, which implies that SHP-1 repression by the N-SH2 domain is most likely to involve conformationally mediated inhibition of substrate binding (16). Molecular dynamics simulation for SHP-2 also identified that the conformational flexibility of the C-terminal half of the N-SH2 domain that interacts with the PTP domain was significantly larger in the absence of phosphopeptide ligand than that in the ligand-complexed N-SH2 domain (24). Homology in both primary and three-dimensional structures of SHP-1 and SHP-2 suggests a similar mechanism of the interaction between the N-SH2 and PTP domains.

Structural Comparison with SHP-2—Determination of the crystal structure of SHP-1 revealed that its three domains are similarly assembled to those in SHP-2 (16). High structural similarity was observed between SHP-1 and SHP-2, especially in the PTP and N-SH2 domains (Fig. 3, *B* and *C*). Superimposition of the N-SH2 domains of SHP-1 and SHP-2 produced an r.m.s. deviation of only 1.3 Å for their Cα atoms. The interactions between the N-SH2 and PTP domains defined from the structure support the previously proposed regulatory mechanism that both SHP-1 and SHP-2 use the N-SH2 domain to keep the enzyme in the inactive conformation (2, 25, 26).

However, the C-SH2 domain in SHP-1 structure is not only differently orientated from that in SHP-2, but its secondary structure elements are relatively more openly organized. The additional superimposition of the C-SH2 domains of SHP-1 and SHP-2, following the superimposition of their N-SH2 and PTP domains (Fig. 3*A*), revealed an up to 56.3-degree rotation of their orientations and a 17.1-Å translation of their mass centroids (Fig. 3*D*). Consequently, the phosphotyrosine-binding pocket (27) of the C-SH2 domain undergoes wide ranging rotation.

The conformation of the N-SH2 domain in SHP-1 appears changed compared with the complex structure of the phosphotyrosine peptide-bound N-SH2 domain of SHP-2. As indicated in Fig. 3*C*, both the Nα2-Nβ7 and Nβ7-Nβ8 loops of N-SH2 domain in SHP-1 project about 5 Å toward the phosphotyrosine-binding pocket and block the binding site for the phosphotyrosine peptide (27). This indicates that stronger interactions exist between the N-SH2 and PTP domains prior to the binding of phosphotyrosine peptide to the N-SH2 domain.

Activation Mechanism of SHP-1—The presence of multiple SH2 domains leads to a problem of the selectivity on phosphopeptide ligands (19). Earlier studies established that N-SH2 domain in SHPs plays more critical role than C-SH2 domain in signaling; however, the C-SH2 domain is indispensable for optimal signaling (2). Although structural comparison of the C-SH2 domains of our ligand-free structure with the peptide-bound C-SH2 domain of SHP-2 provided no direct information about its function, the observed structural differences may suggest that the C-SH2 domain is responsible for searching for the enzyme activator. Together with the special assembly of these three domains, a model was proposed the activation mechanism for SHP-1 (Fig. 4). In this model, the highly mobile C-SH2 domain functions as an antenna to search for phosphopeptides. Binding of phosphopeptide to the C-SH2 domain results in large conformational changes that restore the distorted conformation of the neighboring N-SH2 domain and subsequently opens up its phosphopeptide-binding pocket to harbor a second phosphopeptide molecule. These events can weaken the auto-inhibiting interaction on the interface between the N-SH2 and PTP domains and permit the subsequent synergistic opening up of the active site of the PTP domain. This mechanism is consistent with the notion that a truncated SHP-1 lacking the C-SH2 domain would be activated to a much lesser extent than full-length SHP-1 (25, 26). It also is envisioned that a much larger change in the relative positions of the two SH2 domains will occur due to the mobility of the C-SH2 domain when they are simultaneously bound by biphosphorylated peptides, which can lead to greater movement of the N-SH2 domain. This movement should optimize the opening up of the active site of the PTP domain and can qualitatively explain why biphosphorylated peptides can activate SHPs at a 10-fold higher level than monophosphorylated peptides (28).

Although we have already had the basic concepts of the differentiation and cooperation of these three domains based on the crystallographic and biochemical data, many questions still remain unclear for SHPs. Sequence analysis and structural comparison have revealed highly similar primary and three-dimensional structures of these two C-terminal truncated enzymes. In addition, the C-terminal truncated SHP-1 and the C-terminal truncated SHP-2 could both be activated in an identical manner to their corresponding wild-type enzymes. Nevertheless, although both have the similar phosphorylation sites, the C-terminal tails (~66 residues) of the full-length SHPs share very low sequence homology (<15%), in contrast to the overall high homology (60%). Biochemical and immunological studies showed that the tails are associated with the lipid-binding and subcellular localization of these enzymes (29–30). Therefore, further crystallographic and biochemical studies will be required to understand how the tails regulate the functions of these enzymes and how to cooperate with the other three domains.

REFERENCES

1. Neel, B. G., and Tonks, N. K. (1997) *Curr. Opin. Cell Biol.* **9,** 193–204
2. Barford, D., and Tonks, N. K. (1998) *Structure (Lond.)* **6,** 249–254
3. Tamir, I., Dal Porto, J. M., and Cambier, J. C. (2000) *Curr. Opin. Immunol.* **12,** 307–315
4. Kuriyan, J., and Cowburn, D. (1997) *Annu. Rev. Biophys. Biomol. Struct.* **26,** 259–288
5. Cohen, G. B., Ren, R., and Baltimore, D. (1995) *Cell* **80,** 237–248
6. Famiglietti, S. J., Nakamura, K., and Cambier, J. C. (1999) *Immunol. Lett.* **68,** 35–40
7. Christensen, M. D., and Geisler, C. (2000) *J. Immunol.* **51,** 557–564
8. Wang, L. L., Blasioli, J., Plas, D. R., Thomas, M. L., and Yokoyama, W. M. (1999) *J. Immunol.* **162,** 1318–1323
9. Bouchard, P. Zhao, Z., Banville, D., Dumas, F., Fischer, E. H., and Shen, S. H. (1994) *J. Biol. Chem.* **269,** 19585–19589
10. Su, L., Zhao, Z., Bouchard, P., Banville, D., Fischer, E. H., Krebs, E. G., and Shen, S. H. (1996) *J. Biol. Chem.* **271,** 10385–10390
11. You, M., and Zhao, Z. (1997) *J. Biol. Chem.* **272,** 23376–23381
12. Yu, Z., Su, L., Hoglinger, O., Jaramillo, M. L., Banville, D., and Shen, S. H. (1998) *J. Biol. Chem.* **273,** 3687–3694
13. Liang, X., Meng, W., Niu, T., Zhao, Z., and Zhou, G. W. (1997) *J. Struct. Biol.* **120,** 201–203
14. Otwinowski, Z., and Minor, W. (1997) *Methods Enzymol.* **276,** 307–326
15. Collaborative Computational Project, Number 4 (1994) *Acta Crystallogr. Sect. D Biol. Crystallogr.* **50**, 760–763
16. Hof, P., Pluskey, S., Dhe-Paganon, S., Eck, M. J., and Shoelson, S. E. (1998) *Cell* **92,** 441–450
17. Brunger, A. T., Adams, P. D., Clore, G. M., DeLano, W. L., Gros, P., Grosse-Kunstleve, R. W., Jiang, J. S., Kuszewski, J., Nilges, M., Pannu, N. S., Read, R. J., Rice, L. M., Simonson, T., and Warren, G. L. (1998) *Acta Crystallogr. Sect. D Biol. Crystallogr.* **54,** 905–921
18. Roussel, A., Fontecilla-Camps, J. C., and Cambillau, C. (1990) *Acta Crystallogr. Sect. A* **46,** C66
19. Shakespeare, W. C. (2001) *Curr. Opin. Chem. Biol.* **5,** 409–415
20. Huyer, G., and Ramachandran, C. (1998) *Biochemistry* **37,** 2741–2747
21. Yang, J., Chen, Z., Niu, T., Liang, X., Zhao, Z. J., and Zhou, G. W. (2000) *J. Biol. Chem.* **275,** 4066–4071
22. Yang, J., Liang, X., Niu, T., Meng, W., Zhao, Z., and Zhou, G. W. (1998) *J. Biol. Chem.* **273,** 28199–28207
23. Yang, J., Chen, Z., Niu, T., Liang, X., Zhao, Z. J., and Zhou, G. W. (2001) *J. Cell. Biochem.* **83,** 14–20
24. Wieligmann, K., De Castro, L. F. P., and Zacharias, M. (2002) *In Silico Biol.* **2,** 0028
25. Pei, D., Neel, B. G., and Walsh, C. T. (1993) *Proc. Natl. Acad. Sci. U. S. A.* **90,** 1092–1096
26. Pei, D., Wang, J., and Walsh, C. T. (1996) *Proc. Natl. Acad. Sci. U. S. A.* **93,** 1141–1145
27. Eck, M. J., Pluskey, S., Trub, T., Harrison, S. C., and Shoelson, S. E. (1996) *Nature* **379,** 277–280
28. Pluskey, S., Wandless, T. J., Walsh, C. T., and Shoelson, S. E. (1995) *J. Biol. Chem.* **270,** 2897–2900
29. Craggs, G., and Kellie, S. (2001) *J. Biol. Chem.* **276,** 23719–23725
30. Frank, C., Keilhack, H., Opitz, F., Zschornig, O., and Bohmer, F-D. (1999) *Biochemistry* **38,** 11993–12002
31. Kraulis, P. J. (1991) *J. Appl. Crystallogr.* **24,** 946–950
32. Merritt, E. A., and Bacon, D. J. (1997) *Methods Enzymol.* **277,** 505–524
33. Nicholls, A., Bharadwaj, R., and Honig, B. (1993) *Biophys. J.* **64,** A166
34. Evans, S. V. (1993) *J. Mol. Graph.* **11,** 134–138